Engineering Applications of Artificial Intelligence 112 (2022) 104852

Contents lists available at ScienceDirect

Engineering Applications of Artificial Intelligence

journal homepage: www.elsevier.com/locate/engappai

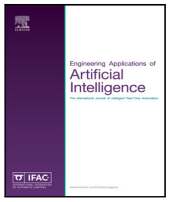

An evolutionary multi-objective path planning of a fleet of ASVs for patrolling water resources

Samuel Yanes Luis [a], Federico Peralta [a], Alejandro Tapia Córdoba [b], Álvaro Rodríguez del Nozal [c], Sergio Toral Marín [a], Daniel Gutiérrez Reina [a,*]

[a] Department of Electronic Engineering, Universidad de Sevilla Sevilla, Camino de Los Descubrimientos, s/n, Sevilla, 41009, Spain
[b] Department of engineering, Universidad Loyola, Av. de las Universidades, s/n, Dos Hermanas, 41704, Spain
[c] Department of Electrical Engineering, Universidad de Sevilla, Camino de Los Descubrimientos, s/n, Sevilla, 41009, Spain

ARTICLE INFO

Keywords:
Autonomous surface vehicles
Water monitoring
Genetic algorithm
Patrolling problem
Multi-objective optimization

ABSTRACT

The rapid increase of human activities with direct influence on the environment has motivated the global awareness of the need to efficiently monitor the natural resources. Among the wide range of problems addressed, such as overuse of agrochemicals, uncontrolled waste, etc., the contamination of water resources plays a protagonist role, given its close links with biodiversity and the food chain. Water monitoring is considered one of the most efficient ways to deal with these problems, especially through the use of autonomous vehicles, which can boost the capabilities and efficiency of the monitoring routines with appropriate strategies. In this work, the monitoring problem is addressed by means of the Non-Homogeneous Patrolling Problem with closed circuits. This problem has a great computational complexity, especially when multiple targets are included in a monitoring mission. A formulation based on closed metric graphs and the application of a multi-objective genetic algorithm is proposed to provide Pareto-efficient monitoring solutions for a variable number of Autonomous Surface Vehicles. To address the multi-agent, multi-objective and constrained paradigm, efficient genetic operators have been designed for the generation of valid solutions in an affordable time. The method results in Pareto-efficient solutions for scenarios with disjoint and uncorrelated objectives, which outperform the fitness of other solutions by a factor of 2, on average. The results provide decision makers a method to find different non-dominated strategies depending on the monitoring needs, depending on fleet and vehicle size.

1. Introduction

Adequate water monitoring constitutes the first step towards an efficient management of natural resources. During the last decades, several human activities and interventions, such as uncontrolled disposal of contamination agents, massive tourism, bad practices in cattle raising, and agriculture, or industrial activities, have put at risk most of the large water bodies around the world (Lin et al., 2021). It is in this context where technology can play an important role to develop robust and efficient monitoring systems and lead a global paradigm shift towards a better use of the natural resources. Water monitoring systems have traditionally relied on manual procedures, generally based on *in situ* acquisition and latter laboratory analysis of collected samples. Yet, they are time and human resource consuming procedures, given the required time for taking samples in different locations of water resources (especially aggravated in large-scale water resources), and for transporting the samples from the water resources to the laboratory. Not only are the monitoring tasks not able to be performed on a real-time basis, but also technicians assume a high risk in extreme scenarios where contamination levels are high. These issues, coupled with an increasing environmental awareness around the world, have caused a noticeable interest in novel monitoring systems aiming at (i) reducing human intervention and (ii) increasing the efficiency of sample collection and further analysis (Jiang et al., 2020; Ighalo et al., 2021; Arzamendia et al., 2016).

Among the different alternatives, the use of Autonomous Surface Vehicles (ASVs) has been gaining momentum lately not only as an efficient alternative to manual sampling for water monitoring tasks (Sánchez-García et al., 2018), but also for related problems such as informative path planning (Peralta Samaniego et al., 2021) and patrolling (Arzamendia et al., 2019a; Yanes et al., 2020), among others. ASVs are cheaper and smaller than conventional ships and can be controlled remotely. Moreover, they can be equipped with sensor probes (pH, conductivity, turbidity, etc.), allowing to carry out monitoring missions

* Corresponding author.
E-mail address: dgutierrezreina@us.es (D.G. Reina).

https://doi.org/10.1016/j.engappai.2022.104852
Received 18 October 2021; Received in revised form 28 January 2022; Accepted 24 March 2022
Available online xxxx
0952-1976/

autonomously in aquatic scenarios (Arzamendia et al., 2016). A relevant aspect of these vehicles lies in the possibility of working on a fleet or swarm basis, sharing the payload of the monitoring missions and thus significantly reducing the time required for accomplishing them. Furthermore, they can work either in a centralized way or in a distributed manner, which dramatically increases their versatility and capabilities.

Despite the chosen strategy, the use of ASVs for water monitoring tasks requires the calculation of sequential sets of waypoints for the vehicles to move through the water resource and carry out the missions. This paper addresses the so-called patrolling problem monitoring task, and more specifically the Non-Homogeneous Patrolling Problem (NHPP). Generally, the patrolling problem for monitoring a water resource is based on its periodical survey to determinate the state of one or several quality indicators through sampling certain physical variables. If all zones of the scenario are considered equally important, that is, they all must be measured with the same frequency, the problem is known as the Homogeneous Patrolling Problem (HPP) (Yanes et al., 2020). In contrast, if different levels of importance or interest are considered, the problem is categorized as NHPP.

Since the NHPP is an extremely complex problem contained in the NP-Hard due to the exploding number of possible combinations, metaheuristic algorithms, such as Genetic Algorithms (GAs) (Whitley, 1994), Swarm Intelligence (Altan and Parlak, 2020), or Reinforcement Learning techniques (Sutton and Barto, 2018) have been proven suitable alternatives. In this work, the NHPP is extended by considering multiple water quality parameters that are required to be monitored simultaneously. Each of these parameters is expected to have an arbitrary distribution through the water resource, and therefore a multi-objective strategy is necessary to determine the optimal policy of the ASVs. A Non-Dominated Sorting GA-II (NSGA-II) is proposed (Deb et al., 2002) in this work. In addition, to encode the movement policy of the different vehicles, a messy representation (Goldberg et al., 1989) is employed for the solutions, as it provides a high flexibility for the generated policies by non-fixing the length of the vehicle's path. The main contributions of this work are:

- Development of a Multi-Objective evolutionary approach based on Pareto dominance and messy individual representation, for the NHPP of water resources.
- Implementation of tailored algorithms to generate, mutate, and crossover domain-constrained individuals using an efficient graph formulation.
- Validation of the proposed approach for multiple vehicles and optimization benchmark functions to model water quality parameters in a real scenario in Paraguay.

The rest of the paper is organized as follows: Section 2 introduces relevant related works that can be found in the current literature, such as the use of both evolutionary approaches and autonomous vehicles for monitoring missions. Section 3 presents the statement of the problem, including the definition of the NHPP and its extension as a multi-objective patrolling problem. Section 4 includes the evolutionary computational approach that has been developed to solve the NHPP. The simulation analysis used to validate the approach is presented in Section 5. Finally, Section 6 summarizes the main conclusions of this paper.

2. Related work

Several artificial-based approaches have been proposed to solve water resources monitoring problems like the Non-homogeneous patrolling problem addressed in this work, such as evolutionary approaches (Arzamendia et al., 2019a, 2016; López Arzamendia et al., 2019; Arzamendia et al., 2019b), reinforcement learning techniques (Yanes et al., 2020; Yanes et al., 2021; Yanes Luis et al., 2021b), swarm optimization (Kathen et al., 2021; Xiong et al., 2019), and Bayesian optimization (Peralta Samaniego et al., 2021; Peralta et al., 2021), among others (Bottarelli et al., 2019).

In Arzamendia et al. (2019a, 2016), the authors solve the homogeneous patrolling or coverage problem of Ypacarai lake by using GAs. The problem is modeled through the classical Traveling Salesman Problem (TSP), by employing visiting points or beacons that are considered to be placed at the shore of the lake. In contrast to the classical TSP, in the proposed problem the objective is for the vehicle to maximize the distance traveled, since it is directly related to the obtained coverage. Due to the high number of possible solutions, and given that the TSP problem is a well-known NP-hard problem, a tailored single objective GA is used. In López Arzamendia et al. (2019), the previous work is extended by modeling the problem using the Chinese Postman Problem (CPP). The number of possible solutions is thus noticeably increased, since the beacons can be visited more than once. Again, the coverage problem is addressed as a single objective problem solved by a GA approach. According to the results, the CPP model outperforms the TSP problem at the cost of increasing the number of possible solutions. In Arzamendia et al. (2019b), a hybrid approach is presented for monitoring water resources. The approach is divided into two steps, (i) an exploration phase based on the TSP presented in Arzamendia et al. (2019a) and (ii) a novel intensification phase. On the one hand, during the exploration phase, the system focuses on finding new areas of the Ypacarai lake that are contaminated. On the other hand, in the intensification phase, the vehicle tries to track the contaminated areas. For both steps, an evolutionary single-objective approach is employed. It is relevant to note that, despite of the robustness of these works, they only address the optimization problem from a single-objective mode.

In Ma et al. (2020), Bezier curves are employed to calculate smooth trajectories in the path planning of a single robot. The objective of the global path planning is to obtain routes that do not contain obstacles. The authors propose a single objective GA with a binary encoding to address this problem. In a similar manner, in Altan (2020) GAs are used for to develop the so-called Swarm Intelligence Algorithms for the optimization of controllers in flying vehicles that perform surveillance and/or monitoring tasks.

Specifically, the Patrolling Problem is theoretically analyzed in Chevaleyre (2004) for the homogeneous and multi-agent case of the patrolling problem under multiple algorithms and maps. This work states that the Patrolling Problem can be solved using a TSP modeling and applying an evolutionary approach and/or using Reinforcement Learning (RL). As claimed by the authors, cyclic strategies using a TSP formulation resulted in a better patrolling than the partitioned-based ones, where every vehicle remains inside of a particular domain zone. Nevertheless, this analysis leaves out the non-homogeneous case.

A Deep Reinforcement Learning (DRL) approach for the non-homogeneous patrolling problem of the Ypacarai lake is presented in Yanes et al. (2020). The authors proposed a 2D Convolutional Neural Network (CNN) to approximate the Q table of the policy of a single vehicle. Moreover, the authors proposed a tailored reward function for the target patrolling problem that considers collisions with land and other invalid solutions. A multi-agent extension of the previous work can be found in Yanes et al. (2021), where up to three vehicles are trained to solve the non-homogeneous patrolling problem of the Ypacarai lake. A thorough comparison between GA and deep reinforcement learning for the non-homogeneous patrolling problem of the Ypacarai lake can be found in Yanes Luis et al. (2021b). The authors compare the centralized Deep Q learning proposed in Yanes et al. (2021) and $\mu + \lambda$ GA implementation, for different resolutions of the problem (different complexity) and a fleet composed of up to three vehicles. The obtained results reveal that: (i) as the complexity of the problem increases, the deep learning approach outperforms the GA, (ii) the deep learning approach is very sensible to hyper-parameters used in the CNN architecture, (iii) the GA is easier to tune and achieves robust solutions, and (iv) the deep reinforcement solutions adapt better to possible failures in the vehicles. In Theile et al. (2020), an aerial

vehicle is trained using a CNN to cover zones of interest in a map with obstacles on a landing spot. In Krishna Lakshmanan et al. (2020), a similar DRL approach was used to deal with the CP for cleaning robots with a high number of degrees of freedom. The results showed much better performance than other approaches and suggest DRL is able to optimize numerous tasks at the cost of many environment evaluations.

Regarding Bayesian Optimization (BO), in Peralta Samaniego et al. (2021) the authors evaluate the utilization of BO based on Gaussian Process for informative path planning of the Ypacarai lake. In the informative path planning, the objective is to collect relevant data from the target scenario to model it by means of a regression model. Therefore, informative path planning is usually a previous step of the patrolling problem. The simulation results demonstrate that the MSE achieved decreases significantly with the number of samples taken; therefore, the Gaussian Process regression model is suitable for modeling water quality variables. In Peralta et al. (2021), the authors extend the work to estimate several water quality variables simultaneously with a single vehicle. In Xiong et al. (2019), the authors proposed a Ant Colony Optimization (ACO) approach with Voronoi partitions for informative path planning in ocean scenarios. The authors use tournament techniques for the selection of the Voronoi zones with higher interest.

The proposed approach presents important advantages with respect to previous and related works. First, this paper proposed a novel graph-based formulation for the NHPP that allows to define tailored individual generation and genetic operators (crossover and mutation schemes). This novel formulation allows finding feasible (but not necessarily optimal) solutions to initialize the population to be optimized. When mutating and crossing individuals, the value of the graph-based method shines through, since the individuals resulting from both operators are guaranteed to satisfy the feasibility navigability constraints. Secondly, it can be highlighted that previous works are based on single-objective patrolling problems (Arzamendia et al., 2016; Yanes et al., 2021; Arzamendia et al., 2019a). In this work, on the contrary, several water quality parameters with different map functions are considered simultaneously in the optimization problem. Unlike traditional approaches found in the literature, the functions under study are not correlated at all, which strongly increases the difficulty to achieve satisfactory patrolling results. Finally, this paper considers the path length in two ways: first, as a hard constraint in the cost function and, in a subsequent analysis, as an additional simultaneous objective. This way, the proposed optimization framework deals with variable length chromosomes to find closed paths of different sizes. Thus, this work also covers the need for multi-scale monitoring in the face of different travel time budgets. In summary, all these aspects constitute a proposal of an amendment to the research gaps found in the literature for monitoring water resources with vehicles: multi-objective and multi-agent optimization with closed path constraints.

3. Statement of the problem

The NHPP problem consists in finding the optimal routes that a single or a fleet of vehicles must follow to optimize a certain cost function. In particular, in this paper, a fleet of ASVs equipped with pollution sensors is considered. The objective of each ASV is to monitor the state of a lake by taking samples at different positions. Consequently, the routes covered by the ASVs are determined by the next considerations:

- There are areas of higher importance that require to be visited and sampled with a higher frequency than others.
- An area that has been visited many times has lower interest than others that remain unvisited.

In this paper, several problems are formulated in terms of the number of objectives and the number of vehicles considered. Thus, this section introduces a formal statement of those problems together with the main assumptions and considerations that have been taken into account.

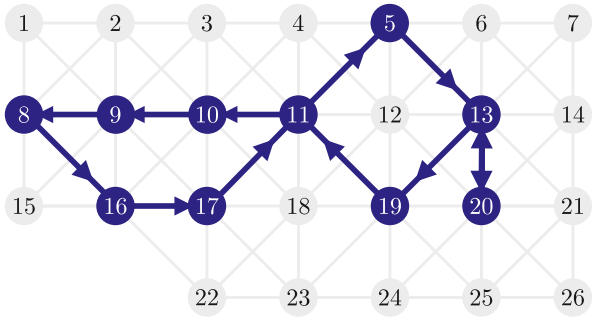

Fig. 1. Example of an arbitrary graph G with 26 nodes and a closed-loop path $P(G) = [16, 17, 11, 5, 13, 20, 13, 19, 11, 10, 9, 8, 16]$. Note that both the nodes and the edges can be visited more than once in a single path.

3.1. Notation and graph-based formulation

Consider a discretization of a certain area defined by a weighted directed graph G in which the vertices of the graph, $V(G) = \{1, 2, \dots, p\}$, represent the set of sectors in which the area has been divided; and the edges of the graph, $E(G) = \{(v_1, v_2) : v_1, v_2 \in V(G)\}$, represent the set of physical paths that interconnects those sectors.

The monitoring criteria for each of the sectors of the lake may vary depending on the local authorities or on how the environmental variables (turbidity, dissolved oxygen, ...) are distributed. Thus, let us define a set $I_e(G) = \{i_{1,e}, i_{2,e}, \dots, i_{p,e}\}$ as the importance of each sector or vertex of the graph to be visited in terms of environmental variable e. In addition, a set $W(G) = \{w_1, w_2, \dots, w_p\}$ defines the idleness of each vertex of the graph. The idleness indicates the number of time steps since the corresponding vertex has not been visited.

Note that, since the position of the vehicles changes at every time step t, the idleness of each vertex also does. Analogously, every time step a certain sector is visited, its corresponding importance decreases. Thus, let us denote as $I_{e,t}(G) = \{i_{1,e,t}, i_{2,e,t}, \dots, i_{p,e,t}\}$ and $W_t(G) = \{w_{1,t}, w_{2,t}, \dots, w_{p,t}\}$ to the importance and idleness sets at step t, respectively.

To have a common base for all objectives of the problem, each variable that denotes the importance of each sector to be visited in terms of an specific environmental variable, $i_{v,e,t}$, takes a normalized value between zero and one. On the other hand, idleness variables $w_{v,t}$ take integer values greater or equal than zero that represent the number of time steps since the vertex v was last visited.

In sight of the above definitions, it is clear that the main aim of each vehicle is to follow a path that visits the most important sectors (those with higher $i_{v,e,t} \in I_{e,t}(G)$) that have been unvisited for a longer time and, consequently, with higher idleness $w_{v,t} \in W_t(G)$. To achieve this combined objective, a variable $\omega_{v,e,t}$ is defined as the relative interest of sector or vertex v in terms of an environmental variable e at time step t:

$$\omega_{v,e,t} = i_{v,e,t} w_{v,t}. \tag{1}$$

which will serve as an indicator of the quality of every action taken.

Once the parameters of the problem have been defined, it is described the variables to be optimized, that is, the paths that the vehicles must follow through the discretized area. The path of a vehicle between vertices v_1 and v_T is defined as a sequence of vertices consecutively visited starting at v_1 and ending at v_T. In the framework of the graph formulation of the problem, a path of a vehicle between vertices v_1 and v_T, $P(G) = [v_1, v_2, \dots, v_T]$, is defined as a vector with the sequence of the T vertices visited during a directed path form vertex v_1 to v_T. In Fig. 1 an example path is represented for the sake of understanding. Recall that a directed path from vertex v_1 to vertex v_T is a sequence of edges such as (v_1, v_2), (v_2, v_3), ..., (v_{T-1}, v_T) in a directed graph. Note that v_t indicates the vertex visited at step t through trajectory $P(G)$.

The relative interest of a vehicle path in terms of an environmental variable e is defined as:

$$\Omega_e(P(G)) = \sum_{v_t \in P(G)} \omega_{v_t,e,t}, \tag{2}$$

where $\omega_{v_t,e,t}$ has been previously defined in (1).

Let $d_{v_1v_2}$ denote the length of edge (v_1, v_2). That is, the distance traveled by the vehicle to move from vertex v_1 to vertex v_2. Then, it can be defined the distance of the path $P(G)$, $D(P(G))$, as the sum of the lengths of all the edges in the direct path defined by $P(G)$. For instance, if the path is defined by $P(G) = [v_1, v_2, \dots, v_T]$, the distance of the path is computed as $D(P(G)) = d_{v_1v_2} + d_{v_2v_3} + \cdots + d_{v_{T-1}v_T}$.

3.2. Single objective and single vehicle patrolling problem

Consider the particular scenario in which the aim of the problem is to optimally design a path $P(G)$ for a single vehicle to maximize the relative interest (2).

Prior to stating the problem, some constraints and considerations must be taken into account:

- Regarding the morphology of every possible path, it is imposed a closed condition for every solution of the NHPP, that is, the starting and ending vertex of the path must be the same.
- To comply with a realistic limited battery constraint of the vehicle, the length of every feasible path $D(P(G))$ must be subjected to a maximum value of traveled distance d_{max}.
- Finally, and in order to model an *attrition* effect to those zones highly covered, the maximum interest of every node in terms of environmental variable e, $i_{v,e,t}$ is reduced a fifth of its original value after every visit. Therefore, a zone that has been covered five times, is not able to contribute to the monitoring task any more.

Considering the above limitations, the optimization problem is formulated as follows:

$$\begin{aligned} \max \quad & \Omega_e(P(G)), \\ s.t. \quad & P(G) = [v_1, v_2, \dots, v_T], \\ & D(P(G)) \le d_{max}, \\ & v_1 = v_T. \end{aligned} \tag{3}$$

3.3. Multi-objective and multi-vehicle patrolling problem

The NHPP can be extended to a multi-objective problem when it is specified that the monitoring of the water resource has more than one interest objective, that is, more than one environmental variable to monitor. In that way, several importance maps $I_e(G)$ are considered. It is important to notice that, when imposing different interest maps, some movements could benefit the maximization of one objective at the sacrifice of the performance in another interest criterion. For example, in Fig. 2, the very same closed path covers different interest levels, and it is clear that the number of possible combinations explodes with the dimension of the map and the number of objectives. This problem constitutes a complex generalization of the NHPP and needs for a multi-objective heuristic approach to balance the monitoring of different variables in a feasible amount of time.

Thereby, the single vehicle multi-objective problem can be formulated as:

$$\begin{aligned} \max \quad & \Omega_{e_1}(P(G)), \Omega_{e_2}(P(G)), \dots, \Omega_{e_N}(P(G)) \\ s.t. \quad & P(G) = [v_1, v_2, \dots, v_T], \\ & D(P(G)) \le d_{max}, \\ & v_1 = v_T, \end{aligned} \tag{4}$$

where N denotes the number of interest maps considered.

It is also possible to expand the problem for a fleet of multiple ASVs. Since the environment is the same for every agent, the graph is consequently shared between them, as shown in Fig. 3. Thus, the objective of a multi-agent fleet is to share the navigable space to monitor better, given the diversity of interests and objectives. Every vehicle will then be able to develop its own path, subjected to the same movement and distance constraints.

$$\begin{aligned} \max \quad & \sum_{n=1}^{N_v} \Omega_{e_1}(P_n(G)), \dots, \sum_{n=1}^{N_v} \Omega_{e_N}(P_n(G)) \\ s.t. \quad & P_n(G) = [v_1^n, v_2^n, \dots, v_{T^n}^n], \quad \forall n \in \{1, \dots, N_v\} \\ & D(P_n(G)) \le d_{max,n}, \quad \forall n \in \{1, \dots, N_v\} \\ & v_1^n = v_{T^n}^n, \quad \forall n \in \{1, \dots, N_v\}, \end{aligned}$$

where N_v defines the number of vehicles and $d_{max,n}$ the maximum distance that vehicle n can cover.

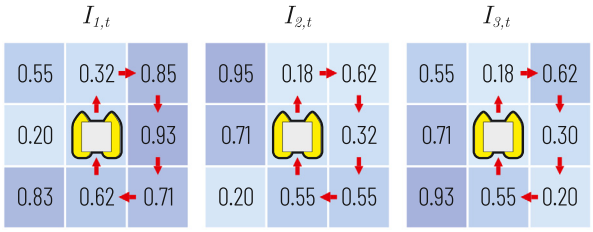

Fig. 2. Example grid graph of a single-vehicle cyclic trajectory with a Multi-Objective interest map. Note that every movement across the graph implies a different value of $\omega_{v,e,t}$.

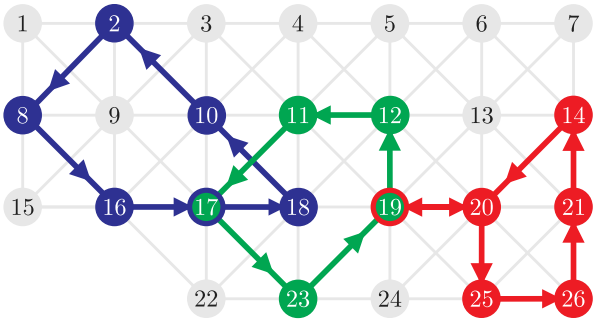

Fig. 3. Example of an arbitrary graph G with 26 nodes and the paths $P_1(G) = [16, 17, 18, 10, 2, 8, 16]$ (blue), $P_2(G) = [23, 19, 12, 11, 17, 23]$ (green) and $P_1(G) = [25, 26, 21, 14, 20, 19, 20, 25]$ (red). Note that both the nodes and the edges can be visited by different vehicles at different steps.

3.4. Complexity of the problem

In Chevaleyre (2004), it is stated and demonstrated that the HPP is contained into the NP-Hard problem set. As the Non-Homogeneous case is a generalization of the former with a non-uniform distribution of the periodicity values for every zone, it is reasonable to categorize the NHPP into the set of NP-Hard problems, which makes exhaustive or brute force algorithms unfeasible. Therefore, the utilization of a GA is a justified approach due to the complexity of the target problem.

3.5. Assumptions and considerations

For evaluation of the proposed patrolling problems, the following assumptions for the movements of the vehicles and the monitoring mission are made:

- At each step, each of the vehicles can perform a single movement that commands the agent to move to one of the adjacent cells, this is moving from a vertex i to a vertex j through an existing edge (i, j).

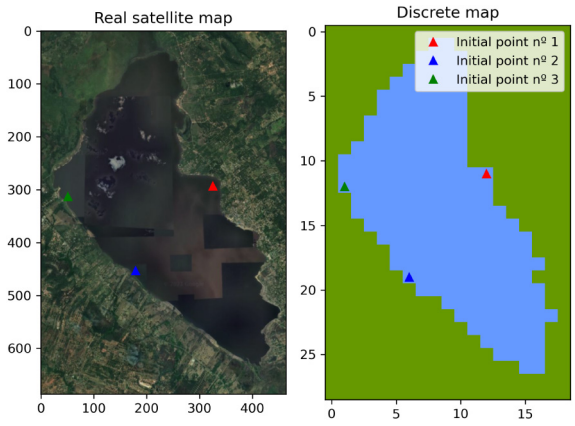

Fig. 4. Satellite image of the YpacaraíLake (left) and the corresponding discrete map used in this approach (right). The triangles indicate the three available deploy points.

- For the sake of simplicity, the map is discretized on a rectangular grid basis, and thus the diagonal movements will have an equivalent cost of the square root of two of a perpendicular movement.
- Each ASV will travel at a nominal speed (2 m/s) with full initial charge (considering a safety minimum for the return to land), on the basis of which the maximum total distance d_{max} (39.5 km) is determined.
- A discrete set of available deployment points are proposed for the ASVs. They correspond to Costa Serena (San Bernardino), Playa Chini (Itauguá), and Playa de Areguá (Areguá) (indicated in Fig. 4). Thus, each ASV must begin and end its path from one of these points.
- Water quality parameters are modeled through optimization benchmark functions (see Section 5). These functions, that are considered to represent water parameters such as pH, temperature, conductivity, turbidity, etc., indicate the quality of the water resource, and are considered to have been obtained in advance by the fleet of vehicles through informative path planning techniques, such as those proposed in Peralta Samaniego et al. (2021) and Kathen et al. (2021).

4. Proposed evolutionary approach

GAs are meta-heuristic optimization algorithms inspired by Darwin's theory of Evolution (Kramer, 2017), which establishes that the better an individual adapts to the environment, the higher its probability of creating offspring and surviving over generations. The robustness and flexibility of these algorithms are such that their popularity has grown exponentially during the last few years, being applied to a wide range of complex engineering problems in very different areas, such as robotics (Kulik and Protopopova, 2020; Ma et al., 2020; Yanes Luis et al., 2021a), energy systems (Ehyaei et al., 2020; Tapia et al., 2020; Alvarado-Barrios et al., 2019), manufacturing processes (Shen et al., 2007; Venkatesan et al., 2009) or structure analysis (Sahu and Nayak, 2020).

The main idea behind a GA is the iterative evolution of a population of candidate solutions (called individuals). Every individual is encoded in a chromosome-like structure (each gene represents a variable of the solution), and then is assigned a fitness value, which measures its adaptation to the search landscape. On the basis of their fitness, certain individuals are stochastically chosen to create new offspring. As a rule, the higher the fitness of an individual, the higher the probability of being chosen as a parent. The new offspring is created by means of crossover and mutation operators. The crossover operator consists of the combination of the genetic information of two individuals, while the mutation consists of modifying certain genetic information of a single individual (both operators are stochastic). Using a proper tuning of the crossover and mutation probabilities, GAs can achieve a good balance between exploration and exploitation within the search landscape of the problem.

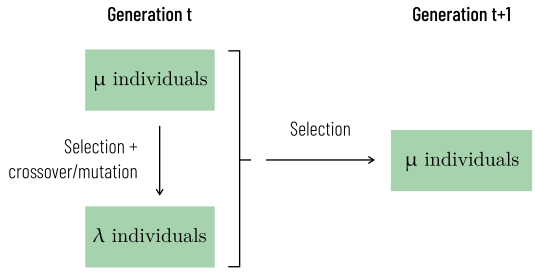

Fig. 5. Working scheme of the $\mu + \lambda$ genetic algorithm.

In this work, each individual represents a possible patrolling plan for a fleet of ASVs, this is, a path for each of the vehicles. Given that the number of movements of a path is not fixed, the algorithm will be formulated as a Messy GA (Goldberg et al., 1989), where the size of the individuals, as will be discussed in Section 4.1, would vary through the generations. Two configurations have been considered to address this work, these are the single and multi-objective modes of the GA.

4.1. Single-objective

The proposed GA is based on $\mu + \lambda$ approach (Ter-Sarkisov and Marsland, 2011). In this algorithm, summarized in Fig. 5, a population of μ individuals compete each other to generate λ children by the genetic operators (crossover and mutation). After evaluating the offspring with the fitness function, the extended population formed by $\mu + \lambda$ individuals compete through the selection scheme used to pass to the next generation. This procedure is repeated until the maximum number of generations is reached. Notice that this approach is more elitist than canonical implementations since parents and children compete.

4.1.1. Individual representation

The encoding of the individuals is proposed to be based on the sequential enumeration of the cells that are visited by each ASV. Given that the length of the paths can vary, an additional gene precedes each of them containing its length. Using T^j to indicate the number of movements that the jth vehicle performs, and v_t^j to indicate the vertex that it visits at the tth step of its path, an arbitrary individual Δ corresponding to a fleet of N_v ASVs would be written in the form of

$$\Delta = \left[T^1, v_1^1, \ldots, v_{T^1}^1, \quad \ldots \quad , T^{N_v}, v_1^{N_v}, \ldots, v_{T^{N_v}}^{N_v}, \right] \tag{5}$$

Two things must be noted regarding the chromosome structure. First, this encoding is generalized for a fleet of any size, that is, for any number of vehicles $N_v \geq 1$. Secondly, it is relevant to highlight that the chromosome has a variable length, as the vehicles can visit a different number of zones during their paths. A representation of the chromosome is shown in Fig. 6 for a better understanding.

4.1.2. Fitness function

For the single-objective mode of the algorithm, the fitness function F is defined as the sum of the total interest collected by the fleet of ASVs, if the paths are feasible. There are two situations that are considered unfeasible, and thus, that cause the individuals to be penalized.

$$F(\Delta) = \begin{cases} \sum_{j=1}^{N_v} \left(\sum_{t=1}^{T^j} \omega_{v_t,e,t} \right) & \textbf{if} \quad \begin{cases} \sum_{t=1}^{T^k-1} \left(d_{v_t^k d_{v_{t+1}^k}} \right) \leq d_{max}, & \forall k \in \{1, \dots, N_v\} \\ v_t^i \neq v_t^j, & \forall n \in \{1, \dots, N_v\}, \forall i, j \in \{1, \dots, T^n\} \end{cases} \\ -1 & \textbf{otherwise} \end{cases} \tag{6}$$

Box I.

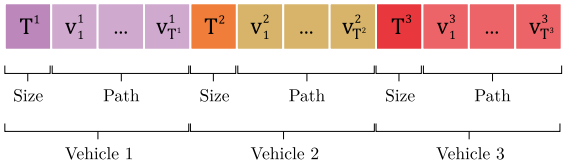

Fig. 6. Scheme of an individual corresponding to a fleet of three ASVs.

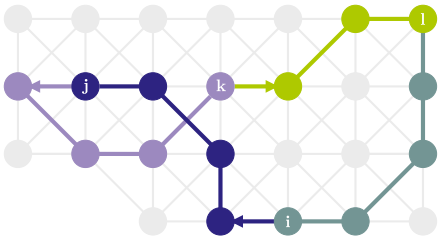

Fig. 7. Example of individual generation with 4 vertex i, j, k, l. The individual is created through the concatenation of the paths connecting each couple of consecutive vertex ($i-j$, $j-k$, $k-l$ and $k-i$). These paths, in different colors, are determined by applying *Dijkstra* algorithm after randomizing the arc-weights.

These are:

1. One or more vehicle's paths exceed the maximum distance traveled, this is, $D(P(G)) \leq dmax$.
2. Two or more vehicles visit the same node v at the same step t.

In both cases, a negative fitness is imposed, which virtually means a death penalty over those individuals. Thus, for any individual Δ in the form of (5), the fitness $F(\Delta)$ can be written as shown in expression (6) is given as in Box I.

4.1.3. Individual generation

In sight of the formulation proposed, it is clear that an individual generation scheme purely based on randomly selecting combinations of vertex $v_i \in V(G)$ with repetitions is not expected to generate feasible individuals correctly. For this reason, a graph-based tailored generation scheme is proposed.

The generation scheme is based on choosing a set of m arbitrary nodes from the graph G and then defining a path $Q(G)$ that visits them consecutively. This path is constructed by successively applying the *Dijkstra* algorithm, with randomized arc weights, to find the shortest path between each node i and the next node $i+1$ from the set, and finally concatenating the resulting path into a single one. Note that, as the generated individual must constitute a closed path, an additional segment, connecting nodes m and 1 from the set is included. In Fig. 7 an example of a generated individual using $m = 4$ nodes is shown.

4.1.4. Genetic operators

To ensure that only feasible individuals are created, tailored algorithms are proposed for mutation and crossover operations. As well as the generation scheme, a graph-based formulation is employed.

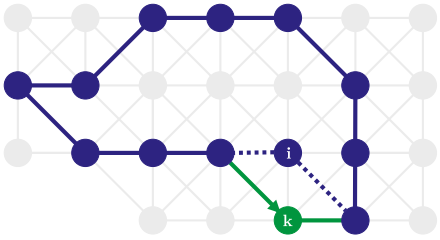

Fig. 8. Example of mutation on an individual. In this example the vertex k steps in for vertex i, which is removed from the original path. Note that only those vertex which are neighbor with both the previous and next visited vertex in the path can be chosen to substitute i.

The mutation operator is based on modifying locally the path of a vehicle, by swapping a visited vertex with a compatible neighbor. This is applied by first choosing a vertex (gene) randomly from the path of one of the vehicles (if more than one). This vertex is removed from the path, and then a new one, randomly chosen among the common neighbors from the previous and the next vertex visited is inserted, closing again the path (see Fig. 8 for an illustrative example). Given the particularities of the resulting graph, whenever there is no possible neighbor to step in for the removed one, a new vertex (gene) is chosen and the process is repeated.

The crossover operator is designed to combine certain segments of the paths from the parents to create offspring. This operator is based on first selecting two vertices i and j from each parent's chromosome, say i_1, j_1 and i_2, j_2. The corresponding segments, $i_1 - j_1$ and $i_2 - j_2$, are removed from their respective paths. Finally, the path from each parent is closed by a detour covering the segment removed from the other parent (see Fig. 9 for an illustrative example). These detours to connect the open paths to the segments are created by applying *Dijkstra* algorithm after randomizing the arc-weights.

4.2. Multi-objective

For the multi-objective case, the well-known NSGA-II algorithm is used (Deb et al., 2002). In the NSGA-II, a $\mu + \lambda$ approach is employed to create an extended population through selection and genetic operators (see Fig. 10). Then, the extended population is sorted by Pareto dominance, placing at the first level those solutions that are dominant. The next step consists of selecting the μ best individuals according to the Pareto-based ranking. In the case that all individuals of the last level cannot pass to the next generation (μ size is the limit), a distance metric is employed to preserve diversity in the Pareto front (see Deb et al. (2002) for more details).

4.2.1. Individual representation

The same individual representation for the single objective mode (Section 4.1) is used.

$$F(\Delta) = \begin{cases} \left(\sum_{j=1}^{N_v} \left(\sum_{t=1}^{T^j} \omega_{v_t,e_1,t} \right), \ldots, \sum_{j=1}^{N_v} \left(\sum_{t=1}^{T^j} \omega_{v_t,e_N,t} \right) \right) & \textbf{if} \quad \begin{cases} \sum_{t=1}^{T^k-1} \left(d_{v_t^k d_{v_{t+1}^k}} \right) \leq d_{max}, & \forall k \in \{1, \ldots, N_v\} \\ v_t^i \neq v_t^j, & \forall n \in \{1, \ldots, N_v\}, \forall i, j \in \{1, \ldots, T^n\} \end{cases} \\ -1 & \textbf{otherwise} \end{cases} \tag{7}$$

Box II.

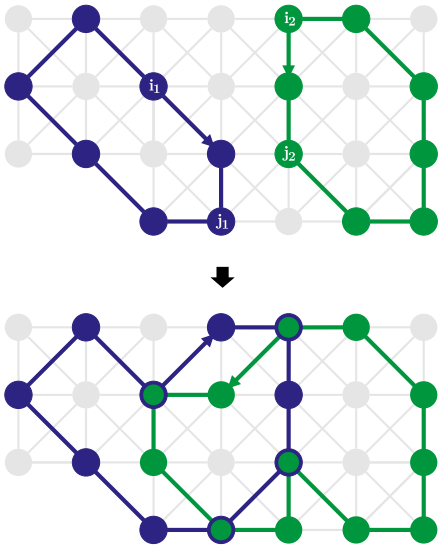

Fig. 9. Example of a crossover between two arbitrary individuals. Segments $i - j$ are randomly chosen and removed for each of the parents. Each of the resulting open-loop paths are closed by a detour that includes the segment removed from the other one.

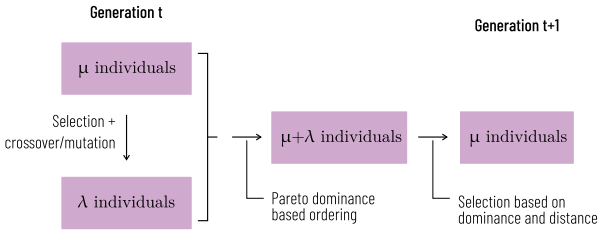

Fig. 10. Working scheme of the NSGA-II genetic algorithm.

4.2.2. Fitness function

The fitness function is defined as maximizing simultaneously the collected relative interest $\omega_{v,e,t}$ corresponding to each of the N importance maps considered, as shown in expression (7) is given as in Box II.

The penalty for individuals that violates the restriction of the problems is again the same as in Section 4.1.2.

4.2.3. Individual generation

The generation scheme proposed for the single objective mode (Section 4.1) is used.

4.2.4. Genetic operators

Both the mutation and crossover tailored operators from the single objective mode (Section 4.1) are used.

5. Simulation results

This section describes the experimental results obtained in the simulations. The conducted simulations are divided into two cases. On the one hand, the problem of a single objective is addressed, which will serve to obtain a baseline of the algorithm with a single interest map (Shekel) with 1–3 ASVs. Furthermore, for this first approximation, a grid-search of parameters (crossover and mutation probability) has been performed for the subsequent experiments. In addition, the proposed approach has been compared with other techniques such as lawnmower and randomized algorithms. On the other hand, a set of experiments has been conducted that deals with the multi-agent case with three objective functions based on typical benchmark functions for optimization. These functions (see Fig. 12), such as Shekel,[1] Rosenbrock,[2] and Himmelblau,[3] which have been converted to maps of interest ($\mathcal{I}$), present interesting challenges to balance the non-homogeneous patrolling of the ASVs, as high interest areas in one map coexist with low interest in others. Thus, these functions are not correlated with each other. Consequently, it is not surprising to find opposed and disperse solutions in the target domain, since human criteria (tourist interest, ...) and biological models of the lake could be blended. In a later analysis of the multi-objective case, the distance traveled by a single ASV (for simplicity) has been included, as part of the objectives to be maximized. Thus, the traveled distance goes from being a constraint to a useful metric in the design of the paths. As a result, it is analyzed how the distance traveled affects the possible set of non-dominated solutions in the three previous objectives.

All simulations have been executed in an Ubuntu Server 18.04, with a 2.24 GHz AMD 16-Core Processor and 64 GB RAM, using Python 3.8.5 and the optimization library DEAP.[4] In order to reduce the computation time, the optimization was parallelized using all the 16 cores of the computer. The code is available for replication purposes.[5] Additionally, an interactive version of the obtained results (Single and Multi-Objective) can be found in the same repository.

5.1. Single-objective simulations

For the single-objective case, 1000 generations of the aforementioned $\mu + \lambda$ algorithm have been computed. This number of generations is sufficient to obtain a good convergence of the GA. In relation to the cross-breed (p_{cx}) and mutation (p_{mut}) operation probabilities, a grid-search of the parameters has been conducted, subjected to $p_{cx} + p_{mut} = 1$ to maintain the population size constant. In every case, the maximum population size is 500 (see Table 1 for a summary of the hyper-parameters). For this single-objective case, the selected objective function is a mapping of the Shekel function with the navigable boundaries of the YpacaraíLake.

In Table 2, the results of the (p_{cx}, p_{mut}) are presented. The achieved results show that for every fleet size, the best tuple of parameters is $(p_{cx}, p_{mut}) = [0.6, 0.4]$. In Fig. 11, the best paths are represented for different fleet sizes. It can be seen that the proposed algorithm is able to optimize the solutions to comply with the restrictions and the target objective function. In the single ASV case, the resulting path puts attention to the most important and close zones to the deploy point

[1] https://www.sfu.ca/~ssurjano/shekel.html.
[2] https://www.sfu.ca/~ssurjano/rosen.html.
[3] https://www.sfu.ca/~ssurjano/stybtang.html.
[4] https://deap.readthedocs.io/.
[5] https://github.com/FedePeralta/EMOPP.

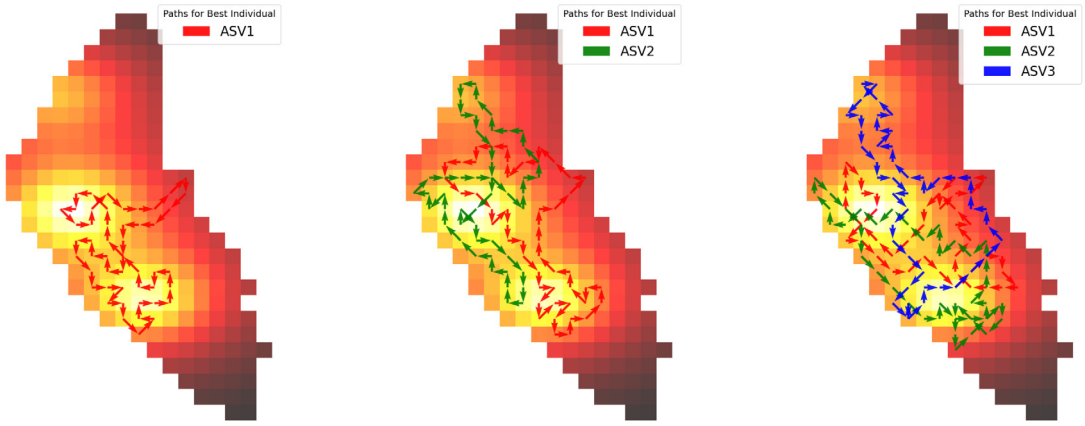

(a) (b) (c)

Fig. 11. Best paths obtained in the single-objective case for (a) 1, (b) 2, and (c) 3 vehicles.

Table 1
Simulation parameters for both the single and multi objective case.

	Single-objective	Multi-objective
μ	500	500
λ	500	500
Generations	1000	1000
Selection	Tournament (size = 3)	NSGA-II
P. Crossover	[0.5, 0.6, 0.7, 0.8]	0.6
P. Mutation	[0.5, 0.4, 0.3, 0.2]	0.4

Table 2
Results of the tests proposed to tune (p_{cx}, p_{mut}) for the single-objective case.

	Hyper-parameter			
p_{cx}, p_{mut}	0.5, 0.5	0.6, 0.4	0.7, 0.3	0.8, 0.2
1 ASV				
Mean	891.90	899.37	901.34	894.12
Std. dev.	31.96	41.28	34.46	37.30
Min	827.15	796.73	823.60	827.15
Max	950.35	**1007.64**	992.46	**1007.64**
2 ASVs				
Mean	1439.79	1455.72	1456.84	1442.15
Std. dev.	51.20	54.86	52.07	62.27
Min	1352.81	1342.34	1288.97	1316.37
Max	1550.92	**1586.10**	1553.78	1556.51
3 ASVs				
Mean	1776.38	1778.09	1772.17	1784.44
Std. dev.	65.51	62.55	61.58	46.89
Min	1627.12	1676.80	1647.42	1674.0
Max	1912.3	**1961.63**	1921.88	1883.67

available and, once those are covered, the vehicle returns using the most informative way found.

When addressing the use of multiple-ASV, it is remarkable how, despite the growing complexity, the algorithm is able to synthesize effective paths for the patrolling task. It is noticeable that the resulting solutions deal not only with the informativeness of the paths (maximization of the base information value $\mathcal{I}$), but also with the fact that revisiting a zone has a very little effect on the fitness during a certain amount of time because of the idleness level $\mathcal{W}$. It can be noticed that the maximum fitness in every NHPP is upper-bounded because of the imposed value of attrition (as explained in Section 3). Hence, adding more ASVs to the patrolling could increase the relative interest collected $\mathcal{I}$ but only up to a certain point. Thus, the saturation of surveillance is translated into a high frequency of visiting due to the high number of agents. This makes the problem even more challenging since adding more ASVs reduces the improvement margin. Therefore, the simulation results included in Table 2 show that the increment of reward with every ASV added is 57.4% in the 2-ASV case and 23,67% in the 3-ASV case, which reflects the attrition property of this problem.

Two notable aspects of these results are: (i) the length of the solution routes and (ii) the merit allocation of the total reward in each ASV. In the former case, it can be observed that the mean distance of the best individuals is 39.06 km, with a standard deviation of 0.3 km, clearly indicating that the longest routes provide the most information in terms of patrolling. Regarding the fitness contribution of each vehicle, when two and three ASVs intervene, on average, the fitness apportionments are [703.72, 746.63] and [572.26, 625.85, 575.18], respectively. Since the reward collected by each vehicle is similar in each case, it is reasonable to state that the algorithm is able to distribute the monitoring capacity homogeneously among them. This quality is especially important, since an imbalance of the workload between vehicles means poor monitoring on inefficient routes and excessive time and battery cost on longer and more effective routes. Furthermore, according to the obtained results, a relevant consideration with respect to the initial points of the agents can be stated: on average, the vehicle that accumulates the most reward in this multi-agent experiment is the ASV starting at initial point 2 from Fig. 4, which gives an idea of the best deployment point.

By comparing the best paths synthesized by the proposed algorithm with other approaches, it is possible to have an idea of how competitive it is for this task. The result of the paths resulting from the single-objective optimization of the Shekel function are compared with a Lawnmower algorithm (Yanes et al., 2020) and a random search of 1000 aleatory selected individuals that comply with the restrictions. In Table 3, it can be observed the proposed optimization scheme allows, on average, a fitness 2.41 times bigger respect to the former, and 1.72 times bigger respect to the latter. This is, consequently, a significant amelioration from classic coverage paths in this particular patrolling problem.

5.2. Multi-objective simulations

Regarding the Multi-Objective problem, the algorithm purposes to obtain a Pareto front since there are multiple objectives to be optimized simultaneously. Each solution consists of a non-dominated solution, according to the sum of the total interest locations visited in a single mission. Fig. 12 shows a representation of the three objectives considered.

Table 3
Comparative between different algorithm in the single-objective optimization problem.

	Algorithm	Max. fitness
1 ASV	Proposed	**1007.64**
	Lawnmower	387.01
	Random	601.20
2 ASV	Proposed	**1586.10**
	Lawnmower	536.17
	Random	922.88
3 ASV	Proposed	**1961.63**
	Lawnmower	1163.76
	Random	1097.22

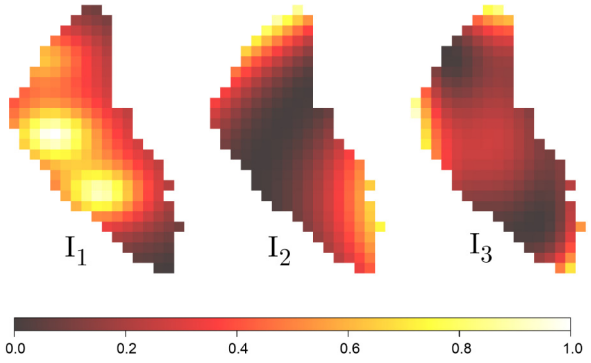

Fig. 12. Three interest maps I considered for the multi-objective approach. Each one is generated using a different benchmark function: Shekel (I_1), Rosenbrock (I_2) and Himmelblau (I_3).

In this Multi-Objective approach, the best set of parameters, used in the previous analysis, (p_{cx}, p_{mut}) is again used. Since the single objective case obtained a good convergence, the same number of generations is employed. The additional parameters involved in this case are also summarized in Table 1.

In Fig. 13, a representation of the obtained results using one vehicle can be observed. It is important to highlight that the resulting Pareto front is neither continuous nor smooth due to the mentioned nonexistent correlation between the used benchmark functions. However, there is a clear adequate behavior in terms of patrolling, which is the objective of this work. Several solutions seem to focus on two objectives and obtain as much as possible of the other, i.e., the yellow to red points obtain high values on Rosenbrock and Himmelblau functions, but fail to achieve a large reward on Shekel function. This situation responds to the impossibility of finding a non-dominant solution that satisfies the Shekel benchmark with the provided distance restriction. In this sense, an expedition of the closed path into the important zones of Shekel function will have little effect on the other objectives. This statement is further supported by observing the left and right-most subfigures in Fig. 13, where the individuals separately focus on the important zones of Rosenbrock (objective shown in middle), and visit one or two important zones of Himmelblau (top). Nonetheless, on overall, the paths fail to visit the peaks and their surrounding zones of Shekel (bottom), which effectively diminishes the reward.

In the cases of fleets of 2 and 3 ships, this behavior is still noticeable, but the objectives seem to be better accomplished. This is mainly due to the fact that there is more available traveling distance (more vehicles). The obtained Pareto front using two vehicles, with the same 3 objectives, is shown in Fig. 14(a). The individuals of this Pareto front seem to highly favor two objectives decreasing the obtained reward of the third. The obtained paths using two vehicles manage to effectively collect reward on high importance zones, but since the available reward of the Shekel function is more spread in the search space, the collected reward is low. Despite this, it is observed that most of the non-dominated solutions provide paths that manage to cover more efficiently the Lake, dividing the patrolling region into two parts. Fig. 14(b) shows this behavior. A very distinct behavior is observed when the fleet has three ships. Fig. 15 shows the Pareto front as well as the paths provided by one of the solutions. In this case, the ships are able to maximize the three objectives simultaneously, with each ship focusing on their surrounding zones rather than the total available search space. A comparison of multi-objective paths with those focused on a single objective (Shekel) can be found in Table 4. With these results, it is clear that the use of a multi-objective approach is justified: the best Pareto dominant solutions on the Shekel axis are a significant improvement over the other objectives. With a 15% loss in the Shekel objective with respect to the Mono-Objective case, the proposed approach obtains a percentage increase of 63% and 1.25% in the other objectives, as a result of the balancing of interest between the fitness maps.

Table 4
Comparative between the fitness of the best individual for the Shekel single objective (SO) optimization applied to other objectives, and the fitness of the maximum non-dominated solution for the multi objective (M) in the Shekel axis.

		Shekel	Rosenbrock	Himmelblau
1 ASV	SO (best)	1007,64	102,90	350,46
	MO	908,03	165,90	379,33
	Inc (%)	−9,89%	61,22%	8,24%
2 ASVs	SO (best)	1586,10	239,53	584,30
	MO	1265,93	306,32	476,37
	Inc (%)	−20,19%	27,88%	−18,47%
3 ASVs	SO (best)	1961,62	426,70	710,82
	MO	1651,38	699,72	719,67
	Inc (%)	−15,82%	63,98%	1,25%

If we delve deeper into the results of the Multi-objective case, it can be seen that the Pareto front representation reflects a sparse and discontinuous solution domain, as mentioned in Section 4. This representation of the non-dominated solutions, grouped in clusters of very different behaviors, serves the designer to choose and visualize patrolling paths when two very similar solutions present a very large divergence in the different objectives (when switching from patrolling the upper part of the map instead of the lower part, for example). If we look at the shape of the Pareto fronts, as we increase the size of the fleet, we can also observe how the solution space becomes more compressed and continuous (even though two clusters of dispersed solutions continue to appear). This phenomenon responds to an increase in the flexibility of the paths to cover significantly more homogeneously the areas of interest. Thus, by studying the average distance of each non-dominated solution to the centroid of all solutions (with their axes normalized) and treating the Pareto front as a hyper-volume (Guerreiro et al., 2020), is it possible to have a measure of how dispersed the solutions are. In the case of the Multi-Objective Scenario, for 1,2 and 3 ASVs, we have an average distance of the solutions of 0.251, 0.197 and 0.108 respectively, indicating that the solution space becomes compressed about 2.5 times from 1 to 3 ASVs.

Finally, considering distance as the fourth objective, Fig. 16 shows the obtained Pareto front using one single ship (for the sake of visualization we have not included the Pareto front for two and three ASVs). In this case, the distance value is represented with the color of every solution in the 3D representation, as indicated by the colorbar. It can be observed that the Pareto front collapses into a single two-move path and becomes increasingly dispersed as the cycles become longer in length. The graphical representation in Fig. 16 allows to understand how the paths are distributed with a limited distance, which can facilitate the designer in multi-objective planning when the cost of battery and time is subject to constraints.

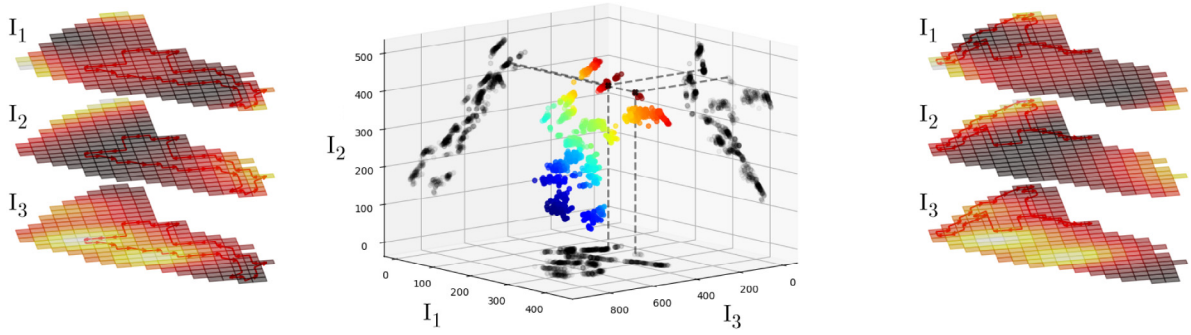

Fig. 13. Representation of the multi-objective problem results, in terms of the objective space (center) and the search space observing two optimal paths (left, right). Note how, despite having the same approximate rewards, both solutions manifest very distinct vehicle behavior. The complete Pareto front-end representation can be found in the form of an interactive tool in the GitHub repository https://github.com/FedePeralta/EMOPP.

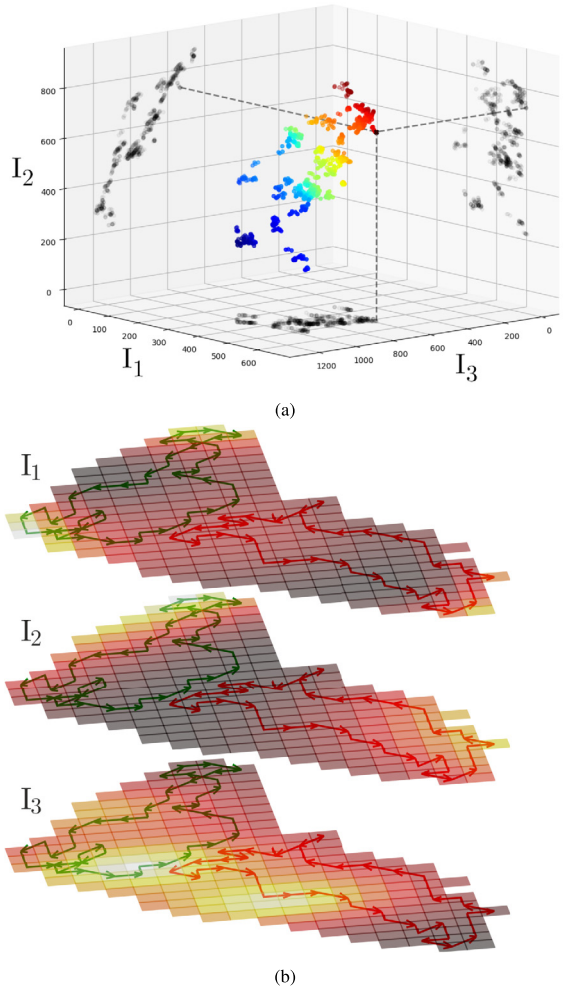

Fig. 14. Representation of (a) Pareto front obtained for two ships with three simultaneous objectives, and (b) paths corresponding to an individual from the Pareto front. Note how in an optimal solution both vehicles clearly divide up the domain of the water resource.

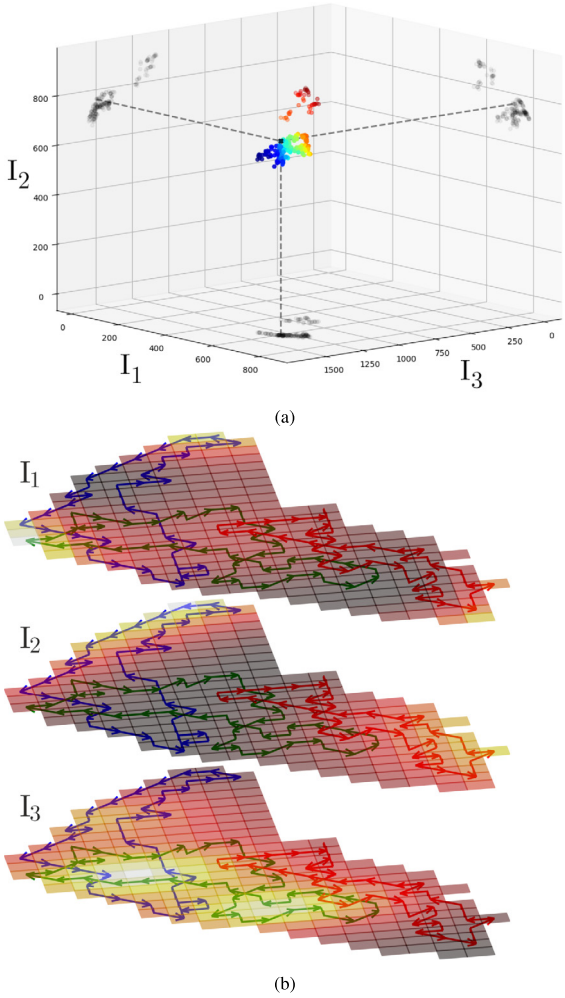

Fig. 15. Representation of (a) Pareto front obtained for three ships with three simultaneous objectives, and (b) paths corresponding to an individual from the Pareto front. Note how making each ASV in charge of a single objective seems an efficient strategy to deal with the multi-objective problem.

5.3. Summary of the simulation results

It is important to note that, as this is a multi-agent and multi-objective problem, the results and solutions require proper discussion and interpretation. With respect to the single objective case, the main results of the analysis conducted are summarized as follows:

- Even though the number of possible solutions is smaller than in the multi-objective case, it is still a challenge to find optimal solutions. For this, it is necessary to perform a hyperparameterization of the crossover and mutation probabilities. It has been

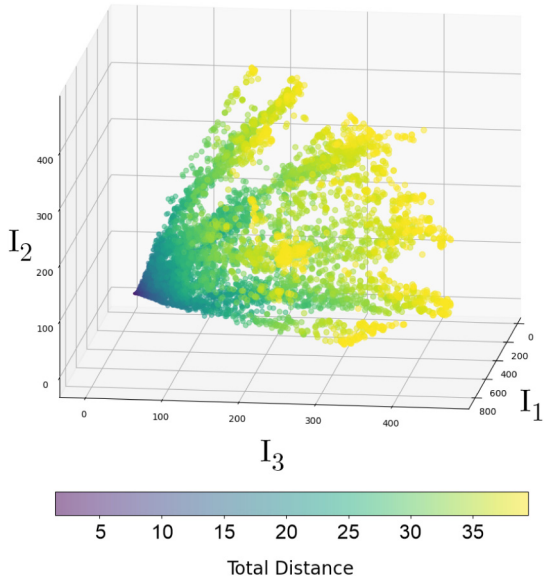

Fig. 16. Representation of the Pareto front obtained for two ships with four simultaneous objectives.

determined that the pair (p_{cx}, p_{mut}) that returns the best solutions is $[0.6, 0.4]$. In any case, it has been observed that it is necessary to perform a hyperparameterization for each problem to be solved.

- In single-vehicle optimization, the solutions are greedy with respect to interest. This makes sense because the vehicle should optimally only make one visit per node, so the effect of attrition does not influence the single-agent case. However, if multiple vehicles are used, the solutions consider both importance and idleness.
- There is a saturation of the reward obtained by the vehicles. Therefore, a lineal increase of the patrolling reward cannot be observed when increasing the size of the fleet. This is a direct effect of the attrition parameter in the patrolling problem.
- For the multi-agent case, the fitness obtained for each vehicle is similar, which indicates that the workload is, too.
- The proposed approach significantly outperforms other algorithms, such as lawnmower and randomized algorithms by a 200%, as a result of the thorough formulation developed.

Regarding the multi-objective case, the main results are:

- For both cases (single-agent a multi-agent), the obtained Pareto fronts are not continuous. This is even more noticeable for a single vehicle case. It is understood that the clustering effect of Pareto-dominant paths occurs because of the very disparate nature of the solutions in the optimization domain, since the objective functions are unrelated to each other.
- The solutions of the Pareto front are observed to only provide satisfactory patrolling results in two out of three considered benchmark functions when one or two vehicles are used. The main reason is that the functions considered are not correlated. Therefore, the interest peaks of I are spread across the scenario, and thus its simultaneous patrolling is impossible. Only with three vehicles, the three benchmark functions can be entirely covered.
- It can be observed that, by increasing the number of vehicles, the Pareto front becomes both more continuous and compressed. The hyper-volume (considering the average distance from its centroid) of the Pareto front decreases from 0.251 (one vehicle) to 0.108 (three vehicles). The reason behind this compression is that the patrolling path, considered as the union of each path of each vehicle, gets larger, thus increasing both the flexibility and the number of possible solutions.
- When the distance is considered as the fourth objective, the number of solutions explodes. As a result, a less dispersed Pareto front can be observed.

6. Conclusions

A novel graph-based formulation has been proposed for the multi-objective non-homogeneous patrolling problem of water resources using autonomous surface vehicles. The proposed approach allows to define tailored genetic operators and an efficient individual generation that achieves satisfactory results in both single-objective and multi-objective cases. The proposed approach has been validated in a simulated scenario of the Ypacarai lake and with up to three benchmark functions (Shekel, Himmelblau and Rosenbrock) that emulate water quality parameters. These functions, which are normally used in optimization algorithm competitions, are not correlated, making it more challenging the multi-objective patrolling problem. The achieved simulation results are good in terms of patrolling reward for the single-objective case, outperforming significantly other competitive approaches. In the multi-objective case, the obtained Pareto front allows the decision makers to evaluate simultaneously dominant solutions in the three objectives with a variable number of vehicles, and also, considering the maximum distance traveled by the vehicles. Therefore, the proposed approach provides an overall picture of the possible solutions in terms of cost considering both the number of vehicles and the battery capacity for the target patrolling problem. As future work, a heterogeneous multi-vehicle system (e.g., air/water) can be used to dynamically allocate tasks according to their advantages and constraints. The proposed system can be also enhanced so that it is able to discover patrolling paths in unknown environments with the use of surrogate models. For future work, it is proposed to study more deeply the dimension of the problem and how complexity can affect the obtaining of optimal solutions. Another future line could be to study how the correlation of the objective functions affects the sparsity of the Pareto set and its implications in terms of speciation within the genetic algorithm.

CRediT authorship contribution statement

Samuel Yanes Luis: Conceptualization, Methodology, Software, Validation, Formal analysis, Writing – original draft. **Federico Peralta:** Conceptualization, Methodology, Software, Validation, Writing – Original draft, Visualization. **Alejandro Tapia Córdoba:** Conceptualization, Methodology, Formal analysis, Writing – original draft, Visualization. **Álvaro Rodríguez del Nozal:** Conceptualization, Methodology, Software, Validation, Formal analysis, Writing – original draft. **Sergio Toral Marín:** Conceptualization, Writing – review & editing, Supervision, Project administration, Funding acquisition. **Daniel Gutiérrez Reina:** Conceptualization, Methodology, Writing – review & editing, Supervision, Project administration, Funding acquisition.

Declaration of competing interest

The authors declare that they have no known competing financial interests or personal relationships that could have appeared to influence the work reported in this paper.

Acknowledgments

This work has been partially funded with under the grant RTI2018-098964-B-I00 funded by MCIN/AEI/ 10.13039/501100011033 and by ”ERDF A way of making Europe”, under the PhD grant FPU-2020 (Formación del Profesorado Universitario) of Samuel Yanes Luis, by the regional government Junta de Andalucía, Spain under the Projects “Despliegue Inteligente de una red de Vehí culos Acuáticos no Tripulados para la monitorización de Recursos Hí dricos US-1257508” and “Despliegue y Control de una Red Inteligente de Vehí culos Autónomos Acuáticos para la Monitorización de Recursos Hí dricos Andaluces PY18-RE0009”.

References

Altan, A., 2020. Performance of metaheuristic optimization algorithms based on swarm intelligence in attitude and altitude control of unmanned aerial vehicle for path following. In: 2020 4th International Symposium on Multidisciplinary Studies and Innovative Technologies (ISMSIT). pp. 1–6. http://dx.doi.org/10.1109/ISMSIT50672.2020.9255181.

Altan, A., Parlak, A., 2020. Adaptive control of a 3D printer using whale optimization algorithm for bio-printing of artificial tissues and organs. In: 2020 Innovations in Intelligent Systems and Applications Conference (ASYU). pp. 1–5. http://dx.doi.org/10.1109/ASYU50717.2020.9259820.

Alvarado-Barrios, L., Rodríguez del Nozal, A., Tapia, A., Martínez-Ramos, J.L., Reina, D., 2019. An evolutionary computational approach for the problem of unit commitment and economic dispatch in microgrids under several operation modes. Energies 12 (11), 2143.

Arzamendia, M., Gregor, D., Reina, D., Toral, S., 2016. Evolutionary path planning of an autonomous surface vehicle for water quality monitoring. In: 2016 9th International Conference on Developments in ESystems Engineering (DeSE). IEEE, pp. 245–250.

Arzamendia, M., Gregor, D., Reina, D.G., Toral, S.L., 2019a. An evolutionary approach to constrained path planning of an autonomous surface vehicle for maximizing the covered area of ypacarai lake. Soft Comput. 23 (5), 1723–1734.

Arzamendia, M., Gutierrez, D., Toral, S., Gregor, D., Asimakopoulou, E., Bessis, N., 2019b. Intelligent online learning strategy for an autonomous surface vehicle in lake environments using evolutionary computation. IEEE Intell. Transp. Syst. Mag. 11 (4), 110–125.

Bottarelli, L., Bicego, M., Blum, J., Farinelli, A., 2019. Orienteering-based informative path planning for environmental monitoring. Eng. Appl. Artif. Intell. 77, 46–58.

Chevaleyre, Y., 2004. Theoretical analysis of the multi-agent patrolling problem. In: IEEE/WIC/ACM International Conference on Intelligent Agent Technology. IEEE, pp. 302–308. http://dx.doi.org/10.1109/iat.2004.1342959.

Deb, K., Pratap, A., Agarwal, S., Meyarivan, T., 2002. A fast and elitist multiobjective genetic algorithm: NSGA-II. IEEE Trans. Evol. Comput. 6 (2), 182–197.

Ehyaei, M.A., Ahmadi, A., Rosen, M.A., Davarpanah, A., 2020. Thermodynamic optimization of a geothermal power plant with a genetic algorithm in two stages. Processes 8 (10), 1277.

Goldberg, D.E., Korb, B., Deb, K., 1989. Messy genetic algorithms: Motivation, analysis, and first results. Complex Syst. 3 (5), 493–530.

Guerreiro, A.P., Fonseca, C.M., Paquete, L., 2020. The hypervolume indicator: Problems and algorithms. arXiv:2005.00515.

Ighalo, J.O., Adeniyi, A.G., Marques, G., 2021. Internet of things for water quality monitoring and assessment: a comprehensive review. In: Artificial Intelligence for Sustainable Development: Theory, Practice and Future Applications. Springer, pp. 245–259.

Jiang, J., Tang, S., Han, D., Fu, G., Solomatine, D., Zheng, Y., 2020. A comprehensive review on the design and optimization of surface water quality monitoring networks. Environ. Model. Softw. 104792.

Kathen, M.J.T., Flores, I.J., Reina, D.G., 2021. An informative path planner for a swarm of ASVs based on an enhanced PSO with Gaussian surrogate model components intended for water monitoring applications. Electronics 10 (13), 1605.

Kramer, O., 2017. Genetic algorithms. In: Genetic Algorithm Essentials. Springer, pp. 11–19.

Krishna Lakshmanan, A., Elara Mohan, R., Ramalingam, B., Vu Le, A., Veerajagadeshwar, P., Tiwari, K., Ilyas, M., 2020. Complete coverage path planning using reinforcement learning for tetromino based cleaning and maintenance robot. Autom. Constr. 112 (May 2019), 103078. http://dx.doi.org/10.1016/j.autcon.2020.103078.

Kulik, S., Protopopova, J., 2020. Genetic algorithm and software tools for solving optimization problems in intelligent robotics. In: Advanced Technologies in Robotics and Intelligent Systems. Springer, pp. 171–178.

Lin, S.-S., Shen, S.-L., Zhou, A., Lyu, H.-M., 2021. Assessment and management of lake eutrophication: a case study in lake erhai, china. Sci. Total Environ. 751, 141618.

López Arzamendia, M.E., Espartza, I., Reina, D.G., Toral, S.L., Gregor, D., 2019. Comparison of Eulerian and Hamiltonian circuits for evolutionary-based path planning of an autonomous surface vehicle for monitoring ypacarai lake. J. Ambient Intell. Humaniz. Comput. 10 (5), 1495–1507. http://dx.doi.org/10.1007/s12652-018-0920-2.

Ma, J., Liu, Y., Zang, S., Wang, L., 2020. Robot path planning based on genetic algorithm fused with continuous bezier optimization. Comput. Intell. Neurosci. 2020.

Peralta, F., Reina, D.G., Toral, S., Arzamendia, M., Gregor, D., 2021. A Bayesian optimization approach for multi-function estimation for environmental monitoring using an autonomous surface vehicle: Ypacarai lake case study. Electronics 10 (8), 963.

Peralta Samaniego, F., Reina, D.G., Toral Marín, S.L., Gregor, D.O., Arzamendia, M., 2021. A Bayesian optimization approach for water resources monitoring through an autonomous surface vehicle: The ypacarai lake case study. IEEE Access 9, 9163–9179. http://dx.doi.org/10.1109/ACCESS.2021.3050934.

Sahu, S., Nayak, B., 2020. An adaptive genetic algorithm method for damage detection in structural elements. Mater. Today Proc. 26, 581–585.

Sánchez-García, J., García-Campos, J., Arzamendia, M., Reina, D., Toral, S., Gregor, D., 2018. A survey on unmanned aerial and aquatic vehicle multi-hop networks: Wireless communications, evaluation tools and applications. Comput. Commun. 119, 43–65. http://dx.doi.org/10.1016/j.comcom.2018.02.002.

Shen, C., Wang, L., Li, Q., 2007. Optimization of injection molding process parameters using combination of artificial neural network and genetic algorithm method. J. Mater Process. Technol. 183 (2–3), 412–418.

Sutton, R.S., Barto, A.G., 2018. Reinforcement Learning: An Introduction. MIT Press.

Tapia, A., Reina, D., Millán, P., 2020. Optimized micro-hydro power plants layout design using messy genetic algorithms. Expert Syst. Appl. 159, 113539.

Ter-Sarkisov, A., Marsland, S., 2011. Convergence properties of two ($\{\mu\} + \{\lambda\}$) evolutionary algorithms on onemax and royal roads test functions. arXiv preprint arXiv:1108.4080.

Theile, M., Bayerlein, H., Nai, R., Gesbert, D., Caccamo, M., 2020. UAV coverage path planning under varying power constraints using deep reinforcement learning. In: 2020 IEEE/RSJ International Conference on Intelligent Robots and Systems (IROS). IEEE, pp. 1444–1449.

Venkatesan, D., Kannan, K., Saravanan, R., 2009. A genetic algorithm-based artificial neural network model for the optimization of machining processes. Neural Comput. Appl. 18 (2), 135–140.

Whitley, D., 1994. A genetic algorithm tutorial. Stat. Comput. 4 (2), 65–85.

Xiong, C., Chen, D., Lu, D., Zeng, Z., Lian, L., 2019. Path planning of multiple autonomous marine vehicles for adaptive sampling using voronoi-based ant colony optimization. Robot. Auton. Syst. 115, 90–103.

Yanes, S., Reina, D.G., Marín, S.L.T., 2021. A multiagent deep reinforcement learning approach for path planning in autonomous surface vehicles: The Ypacaraí lake patrolling case. IEEE Access 9, 17084–17099.

Yanes, S., Reina, D.G., Toral Marín, S.L., 2020. A deep reinforcement learning approach for the patrolling problem of water resources through autonomous surface vehicles: The Ypacarai lake case. IEEE Access 6, 1. http://dx.doi.org/10.1109/ACCESS.2020.3036938.

Yanes Luis, S., Gutiérrez-Reina, D., Toral Marín, S., 2021a. A dimensional comparison between evolutionary algorithm and deep reinforcement learning methodologies for autonomous surface vehicles with water quality sensors. Sensors 21 (8), 2862.

Yanes Luis, S., Reina, D.G., Toral, S., 2021b. A dimensional comparison between evolutionary algorithm and deep reinforcement learning methodologies for autonomous surface vehicles with water quality sensors. Sensors 21 (8), http://dx.doi.org/10.3390/s21082862, URL https://www.mdpi.com/1424-8220/21/8/2862.